



DOI: 10.31636/pmju.v8i1-2.5

## Establishment of a mouse model of stellate ganglion block and subsequent biphasic effects on bilateral cerebral cortical blood flow

Jiahua Wang<sup>1</sup>, Wei Zhou<sup>1,2,3</sup>, Xiaohong Wang<sup>1</sup>, Shiting Yan<sup>2</sup>, Shunping Tian<sup>1,3</sup>, Ying Wang<sup>1</sup>, Yanlong Yu<sup>1,3</sup>, Hu Li<sup>1,2</sup>, Dongsheng Zhang<sup>1,3</sup>, Zhuan Zhang<sup>1</sup>

<sup>1</sup> Affiliated Hospital of Yangzhou University, Yangzhou University, Yangzhou, China;

<sup>2</sup> School of Medicine, Yangzhou University, Yangzhou, China;

<sup>3</sup> Dalian Medical University, Dalian, China

Funding sources: This research was supported by the Medical Key Talents Training Project of the Yangzhou City Health and Family Planning Commission (ZDRC201815) and the Key Program of The Affiliated Hospital of Yangzhou University Research Grant (YZYY2017-07).

Conflicts of interest: The authors declare that they have no conflicts of interest.

### Abstract:

**Background and objectives:** stellate ganglion block (SGB) has significant therapeutic efficacy in various clinical practices and further exploration of SGB is needed. The mouse model of SGB had not been reported and the effect on cerebral cortical blood flow (CCBF) was controversial. We aimed to establish an stellate ganglion block (SGB) mouse model and explore how SGB influences CCBF.

**Methods:** male C57BL/6 mice were randomly divided into five groups ( $n = 6$ ): groups L (left SGB) and R (right SGB) received an injection of 0.25% ropivacaine hydrochloride (0.08 mL) on the respective stellate ganglion; similarly, groups SL (left saline control) and SR (right saline control) received an injection of normal saline (0.08 mL) instead. Group C received no intervention. CCBF was assessed before SGB ( $T_0$ ) and 10 ( $T_1$ ), 30 ( $T_2$ ), 60 ( $T_3$ ), 90 ( $T_4$ ), and 120 min ( $T_5$ ) after SGB using laser speckle contrast imaging system.

**Results:** the SGB mouse model was successfully established in groups L and R. Compared with baseline, CCBF on the blocked side decreased at  $T_1$ , increased at  $T_2$ - $T_5$ , and peaked at  $T_3$  in groups L and R (all,  $P < 0.01$ ). Compared with groups C and SL, the CCBF on the left side decreased at  $T_1$  and increased at  $T_2$ - $T_5$  in group L (all,  $P < 0.05$ ). A similar trend was noted in groups C and SR relative to group R. The CCBF on the unblocked side decreased at  $T_1$ , increased at  $T_2$ - $T_5$ , and peaked at  $T_3$  in groups L and R (all,  $P < 0.01$ ).

**Conclusions:** the SGB mouse model was established successfully. Unilateral SGB can affect bilateral cerebral cortical blood flow, which shows a transitory decrease followed by a significant increase for at least 2 h.

**Key words:** Stellate ganglion block; Mouse model; Cerebral blood flow; Sympathetic nerve system

## Introduction

The stellate ganglion, a star-shaped structure on the cervical-thoracic sympathetic chain, is located at the level of the seventh cervical vertebra and contains neurons that provide sympathetic innervation for the head, neck, heart, cervical thoracic area, and upper limbs. Injecting local anesthetics near the stellate ganglion can temporarily block the conduction of nerve impulses, which is called stellate ganglion block (SGB). SGB has been used widely in pain treatment, such as complex regional pain syndrome<sup>[1]</sup>. Moreover, it also has other clinical indications, including hot flashes<sup>[2]</sup>, sleep disorders<sup>[2]</sup>, arrhythmia<sup>[3]</sup>, and post-traumatic stress disorder syndrome<sup>[4]</sup>.

The mechanisms underlying SGB and wider application of SGB in clinical practice are ongoing matters of investigation. However, clinical research is limited by certain obstacles, such as heterogeneity of patients. Therefore, it is necessary to establish feasible and reproducible animal models of SGB for preclinical studies. The rat models of SGB have been previously reported<sup>[5,6]</sup>. The mouse model has more obvious advantages than the rat model, such as more transgenic, gene knock-out, gene knock-in, and other types of mice and more mice strains are used to establish various experimental animal models. Therefore, establishing an SGB mouse model is extremely important and will help reveal the complex mechanism of action of SGB and expand its therapeutic range.

To our knowledge, there is currently no literature report on the establishment of an SGB mouse model. There is lack of consensus on the role of the sympathetic nervous system in controlling cerebral circulation<sup>[7]</sup>. Notably, experimental evidences demonstrating SGB-induced changes in cerebral cortical blood flow (CCBF) are lacking. The first aim of this study is to explore how an SGB mouse model can be established. The second aim is to investigate the effects of SGB on bilateral CCBF using a laser speckle contrast imaging system. To our knowledge, this study is the first to establish an SGB mouse model and demonstrate subsequent, SGB-induced changes of bilateral CCBF.

## Materials and methods

### Animals

Male C57BL/6 mice (body weight 23–27 g; aged 8–9 weeks) were purchased in the groups of 3 individuals per cage from Comparative Medicine Center of Yangzhou University [Animal production license number:

SCXK (Su) 2017–0007]. The mice were maintained in a 12-h/12-h light/dark cycle-regulated air-conditioned room ( $22^{\circ}\text{C} \pm 1^{\circ}\text{C}$ ). Drinking water and lab chow were made available ad libitum. All experimental procedures were conducted in accordance with the National Institutes of Health Guide for the Care and Use of Laboratory Animals and approved by the experimental animal ethics committee of Affiliated Hospital of Yangzhou University, the suffering and discomfort of animals were minimized as best as possible. To make the mice amenable to the experiments, the mice were handled on a daily basis for 1 week before the experiments.

### Experimental Design

In this study, the mice were divided into five groups with six mice per group using a random number table. In group L (left SGB group) and group R (right SGB group), the mice received an injection of 0.25% ropivacaine hydrochloride on the left and right stellate ganglia, respectively. In group SL (the left-sided saline group) and group SR (right-sided saline group), the mice received an injection of normal saline on the left and right stellate ganglia, respectively. Group C (blank control group) received no intervention.

Protocol of percutaneous posterior approach for stellate ganglion block.

For the animals in groups L and R, anesthesia was induced with 3.5% sevoflurane and maintained with 1.5% sevoflurane through the anesthesia machine (R500, RWD Life Science Co., LTD, Shenzhen, China); the mice were allowed to breathe spontaneously throughout the experiment. Then, their limbs were fixed with a medical adhesive tape in the prone position to make the local structure more recognizable and easily operable. During the entire procedure, their body temperature was maintained at  $37^{\circ}\text{C} \pm 0.5^{\circ}\text{C}$  using a regulated heating pad. After sterilizing the nuchal region using ethanol, the mice were palpated with the process of the 7th cervical vertebra as a prominence. The spinous process was palpated and fastened with the operator's left index finger, and a 1-mL syringe (0.4 × 16, RW SB, Jiangsu Kangjin Medical Equipment Co., LTD, Changzhou, China) with 0.08 mL of 0.25% ropivacaine hydrochloride in it was held in the operator's right hand (Figure 1). The needle was transcutaneously inserted posteriorly, and along the side of the 7th cervical vertebra, it was advanced vertically to a depth of approximately 5 mm from the skin. As soon as the tip of the needle was sensed to have lost contact with the vertebral body, the needle was with-

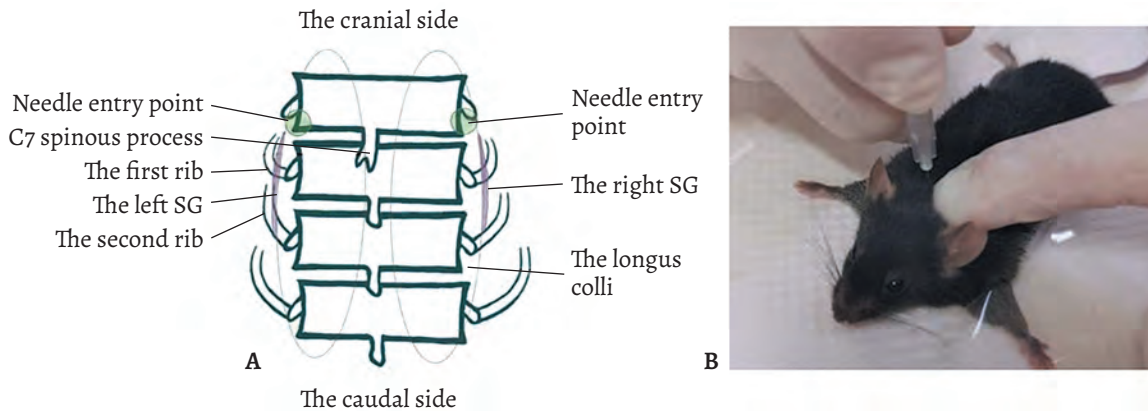


**Fig. 1.** Establishment of percutaneous posterior approach for the SGB mouse model (A) anatomic schematic diagram of stellate ganglion; (B) operation of percutaneous posterior approach for the SGB mouse model SG, stellate ganglion; SGB, stellate ganglion block. Measurements of CCBF by laser speckle contrast imaging system

drawn ~1 mm and kept there while the local anesthetic was injected slowly under the circumstances of no blood or cerebrospinal fluid suctioned out. Notably, the loss of contact of the needle with the vertebral body indicated by a sense of loss of friction between the needle and the vertebra signified that the needle had passed the anterior aspect of the vertebral body. Similarly, mice in groups SL and SR were injected with 0.08 mL of normal saline. As mentioned earlier, mice in group C received no intervention. When mice recovered from general anesthesia, ptosis, the most recognizable feature of Horner's syndrome and an indicator of successful SGB in this study, was recorded.

The anesthetized mice were immobilized in the prone position with their heads fixed on the stereotaxic device using ear bars. The hair on the top of the mice skull was shaved, and then, a median incision was made to expose most of the skull from the front of the frontal bone to the back of the occiput. Then, the periosteum was separated, and the residual hair on the skull were wiped using a cotton swab moistened with normal saline at 37 °C. The laser speckle contrast imaging system (RFLSIII; RWD Life Science Co., LTD, Shenzhen, China) was used to reflect the perfusion of cortical vessels in high spatial resolution mode. CCBF was calculated using a temporal algorithm and recorded consecutively. As shown in Figure 2, the two identical, symmetrically located regions of interest (ROI) between the bregma and lambda were studied separately for evaluating cortical blood perfusion of the two hemispheres. The skull surface was illuminated by scattered light from a 785-nm, 90-mW laser diode while it was covered with a thin layer of 37°C saline solution us-

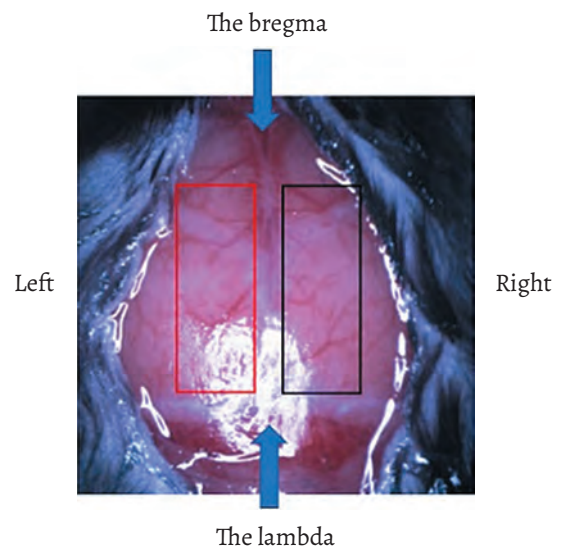


**Fig. 2.** The two identical and symmetrically located regions of interest between the bregma and lambda

ing a soaked cotton swab; the surface was moistened intermittently to improve imaging. The real-time images were acquired continuously every 10 s with an exposure time of 9 ms, generating a total of 18 images over a 3-min period for each time point. CCBF was measured before SGB (baseline,  $T_0$ ) and at 10 min, 30 min, 60 min, 90 min, and 120 min after SGB ( $T_1$ ,  $T_2$ ,  $T_3$ ,  $T_4$ , and  $T_5$ ). The CCBF values of the ROI at the assigned time points were represented by the average blood flow during a 3-min period for each time point. During the procedure, the mice were consistently placed on a regulated temperature heating pad to maintain the body temperature at  $37^\circ\text{C} \pm 0.5^\circ\text{C}$ .

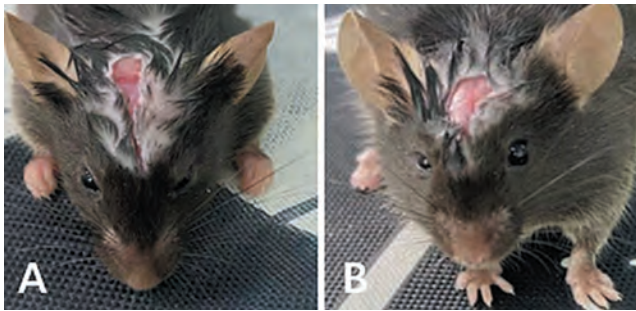


**Fig. 3.** Ipsilateral ptosis after SGB.  
(A) left ptosis after left SGB; (B) right ptosis after right SGB

## Statistical analysis

Statistical software SPSS 19.0 was used for data analysis. Notably, normally distributed data were expressed as mean  $\pm$  standard deviation (SD). The CCBF to the ROI in the left hemisphere (groups L, SL, and C) and the right hemisphere (groups R, SR, and C) was analyzed by one-way repeated-measures analysis of variance (ANOVA), which was followed by the LSD test for multiple comparisons. The CCBF to the ROI in the two hemispheres (group L vs. group R) was also compared using the above method. A  $P$  value of  $< 0.05$  was considered to indicate statistical significance.

## Results

Mice in group L developed left ptosis at about  $49.83 \pm 10.96$  s after SGB, whereas mice in group R developed ipsilateral ptosis at about  $54.83 \pm 9.56$  s after SGB (Figure 3). The duration of onset of ptosis did not significantly differ between the two groups ( $P = 0.419$ ).

None of the mice receiving unilateral SGB developed contralateral ptosis. No ptosis occurred in groups C, SL, and SR.

The basic values of bilateral CCBF did not significantly differ among the groups ( $P_{T_0} = 0.885$  for C vs. SL,  $P_{T_0} = 0.961$  for C vs. L,  $P_{T_0} = 0.847$  for L vs. SL,  $P_{T_0} = 0.603$  for C vs. SR,  $P_{T_0} = 0.555$  for C vs. R,  $P_{T_0} = 0.274$  for R vs. SR). In addition, there were no significant differences in bilateral CCBF among groups C, SL and SR at each time point ( $P_{T_1-T_5} = 0.104, 0.554, 0.45, 0.563, \text{ and } 0.356$  for C vs. SL,  $P_{T_1-T_5} = 0.734, 0.622, 0.591, 0.553, \text{ and } 0.583$  for C vs. SR, respectively).

Compared with  $T_0$ , the CCBF on the blocked side decreased significantly at  $T_1$  (all  $P_{T_1} < 0.001$ ), increased significantly at  $T_2-T_5$  (all  $P_{T_2-T_5} < 0.001$ ), and peaked at  $T_3$  in groups L and R. In groups L and R, the CCBF on the blocked side was significantly higher at  $T_3$  and  $T_4$  than at  $T_2$  and  $T_5$  (all  $P < 0.001$  for  $T_2/T_5$  vs.  $T_3/T_4$ ). CCBF did not significantly differ between  $T_3$  and  $T_4$  ( $P_L = 0.313, P_R = 0.83$ ), while it was significantly higher at  $T_2$  than at  $T_5$  ( $P_L < 0.001, P_R = 0.002$ ).

Compared with groups C and SL, the left CCBF in group L significantly decreased at  $T_1$  and increased at  $T_2-T_5$  ( $P_{T_1} = 0.006$  for L vs. C,  $P_{T_1} < 0.001$  for L vs. SL, and  $P_{T_2-T_5} < 0.001$  for L vs. C/SL). Compared with groups C and SR, the right CCBF in group R significantly decreased at  $T_1$  and increased at  $T_2-T_5$  ( $P_{T_1-T_4} < 0.001$  for R vs. C/SR,  $P_{T_5} = 0.028$  for R vs. C,  $P = 0.009$  for R vs. SR). All of these trends are reflected in Figures 4, 5, 8, and 9.

Compared with the CCBF at  $T_0$ , the CCBF on the contralateral side decreased at  $T_1$  ( $P_{T_1} = 0.019$ ) and increased at  $T_2-T_5$  ( $P_{T_2-T_5} < 0.001$ ) significantly in group L. At  $T_1$ , the decreased degree of the CCBF in group L was signifi-

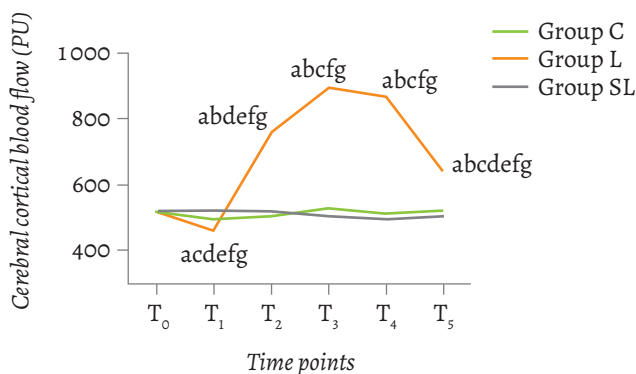


**Fig. 4.** Changes in the left CCBF at each time point in groups C, L, and SL.

<sup>a</sup> Compared with  $T_0$ ,  $P < 0.01$ ; <sup>b</sup> compared with  $T_1$ ,  $P < 0.01$ ; <sup>c</sup> compared with  $T_2$ ,  $P < 0.01$ ; <sup>d</sup> compared with  $T_3$ ,  $P < 0.01$ ; <sup>e</sup> compared with  $T_4$ ,  $P < 0.01$ ; <sup>f</sup> compared with group C,  $P < 0.05$ ; <sup>g</sup> compared with group SL,  $P < 0.05$ ; <sup>h</sup> compared with group SR,  $P < 0.05$ . CCBF, cerebral cortical blood flow;  $T_0$ , baseline;  $T_1$ , 10 min after SGB;  $T_2$ , 30 min after SGB;  $T_3$ , 60 min after SGB;  $T_4$ , 90 min after SGB;  $T_5$ , 120 min after SGB

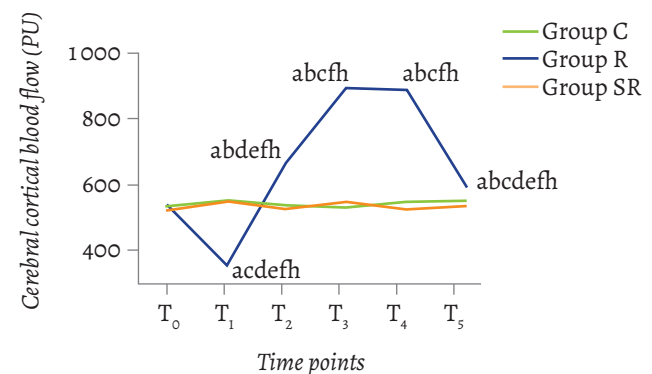


**Fig. 5.** Changes in the right CCBF at each time point in groups C, R, and SR.

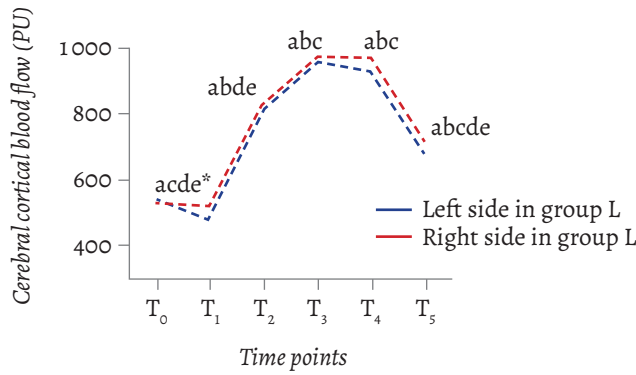


Fig. 6. Changes of bilateral CCBF at each time point in group L.

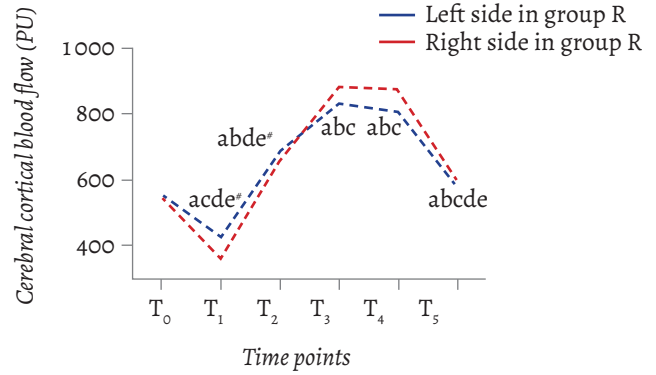


Fig. 7. Changes of bilateral CCBF at each time point in group R.

\* Compared with the left side,  $P < 0.05$ ; \* Compared with the right side,  $P < 0.05$ ; <sup>a</sup> compared with  $T_0$ ,  $P < 0.01$ ; <sup>b</sup> compared with  $T_1$ ,  $P < 0.01$ ; <sup>c</sup> compared with  $T_2$ ,  $P < 0.01$ ; <sup>d</sup> compared with  $T_3$ ,  $P < 0.01$ ; <sup>e</sup> compared with  $T_4$ ,  $P < 0.01$ ; CCBF, cerebral cortical blood flow;  $T_0$ , baseline;  $T_1$ , 10 min after SGB;  $T_2$ , 30 min after SGB;  $T_3$ , 60 min after SGB;  $T_4$ , 90 min after SGB;  $T_5$ , 120 min after SGB

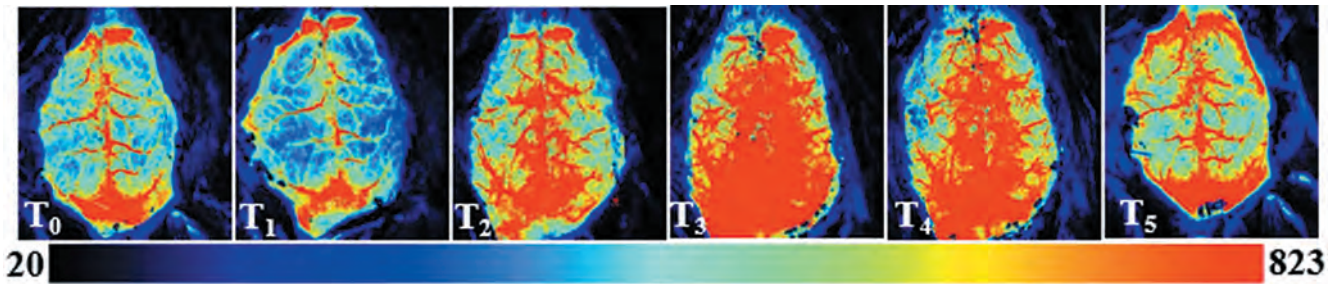


Fig. 8. CCBF images at each time point under laser speckle contrast imaging system in group L.

CCBF, cerebral cortical blood flow.  $T_0$ , baseline;  $T_1$ , 10 min after SGB;  $T_2$ , 30 min after SGB;  $T_3$ , 60 min after SGB;  $T_4$ , 90 min after SGB;  $T_5$ , 120 min after SGB

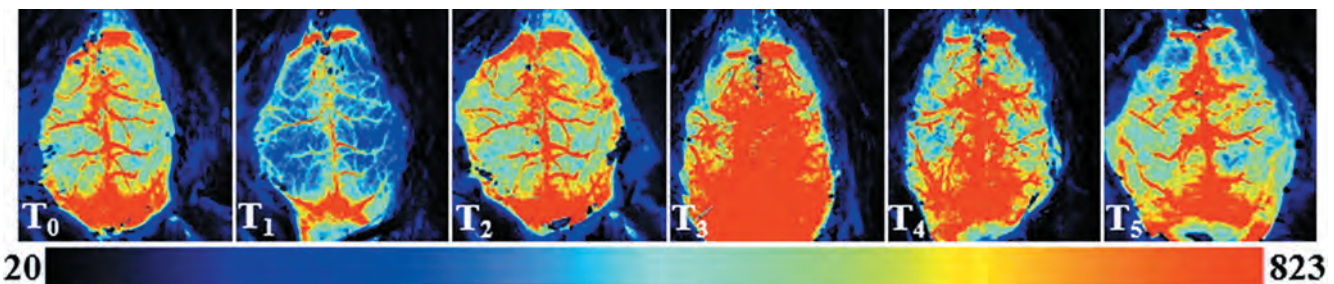


Fig. 9. CCBF images at each time point under laser speckle contrast imaging system in group R.

CCBF, cerebral cortical blood flow.  $T_0$ , baseline;  $T_1$ , 10 min after SGB;  $T_2$ , 30 min after SGB;  $T_3$ , 60 min after SGB;  $T_4$ , 90 min after SGB;  $T_5$ , 120 min after SGB

cantly lower on the right side than on the left side ( $P_{T_1} = 0.004$ ); however, there were no significant differences between the two sides at each time point of  $T_2 - T_5$  ( $P_{T_2-T_5} = 0.263, 0.602, 0.155, \text{ and } 0.059$ , respectively). The trends of bilateral CCBF in group L were consistent, with CCBF being significantly higher at  $T_3$  and  $T_4$  than at  $T_2$  and  $T_5$  ( $P < 0.001$  for  $T_2/T_5$  vs.  $T_3$ ,  $P < 0.001$  for  $T_5$  vs.  $T_4$ ,  $P = 0.001$  for  $T_2$  vs.  $T_4$ ). There were no significant differences in CCBF between  $T_3$  and  $T_4$  ( $P = 0.95$ ), while it was significantly higher at  $T_2$  than at  $T_5$  ( $P < 0.001$ ). Compared with  $T_0$ , the

CCBF on the contralateral side significantly decreased at  $T_1$  ( $P < 0.001$ ) and increased at  $T_2 - T_5$  ( $P_{T_2-T_4} < 0.001$ ,  $P_{T_5} = 0.027$ ) in group R. The decreased degree of CCBF in group R was significantly lower on the left side than on the right side at  $T_1$  ( $P = 0.01$ ); however, there were no significant differences between the two sides at each time point of  $T_2 - T_5$  ( $P_{T_2-T_5} = 0.12, 0.093, 0.056, \text{ and } 0.681$ , respectively). The trends of bilateral CCBF in group R were also consistent, with CCBF being significantly higher at  $T_3$  and  $T_4$  than at  $T_2$  and  $T_5$  (all  $P < 0.001$  for  $T_5$  vs.  $T_3/T_4$  and

**Table 1. Changes in CCBF at each time point in each group**

Group	Side	T <sub>0</sub>	T <sub>1</sub>	T <sub>2</sub>	T <sub>3</sub>	T <sub>4</sub>	T <sub>5</sub>
C	Left	514.92 ± 31.78	498.20 ± 24.21	505.28 ± 35.15	524.48 ± 19.80	511.50 ± 39.84	520.45 ± 21.45
	Right	534.87 ± 34.85	549.77 ± 39.25	532.42 ± 21.71	526.85 ± 42.76	541.99 ± 44.82	546.25 ± 30.58
L	Left	514.22 ± 16.73	459.75 ± 13.71 <sup>acdefg</sup>	760.21 ± 34.17 <sup>abdefg</sup>	891.72 ± 62.31 <sup>abefg</sup>	865.46 ± 35.93 <sup>abefg</sup>	641.34 ± 30.08 <sup>abcdefg</sup>
	Right	511.84 ± 8.07	493.75 ± 18.08 <sup>acde*</sup>	786.06 ± 40.97 <sup>abde</sup>	907.17 ± 32.47 <sup>abc</sup>	905.06 ± 51.90 <sup>abc</sup>	679.49 ± 31.98 <sup>abcde</sup>
SL	Left	517.01 ± 23.17	519.10 ± 23.18	516.43 ± 25.52	505.03 ± 37.29	499.92 ± 24.07	503.08 ± 40.38
	Right	527.06 ± 26.08	517.01 ± 28.34	518.10 ± 26.34	506.70 ± 34.23	525.10 ± 34.09	504.75 ± 42.09
R	Left	544.19 ± 18.34	420.71 ± 30.37 <sup>acde#</sup>	685.78 ± 36.58 <sup>abde</sup>	832.74 ± 38.98 <sup>abc</sup>	802.27 ± 46.11 <sup>abc</sup>	586.03 ± 16.60 <sup>abcde</sup>
	Right	545.65 ± 26.28	357.72 ± 37.68 <sup>acdefh</sup>	657.83 ± 16.72 <sup>abdefh</sup>	883.02 ± 53.54 <sup>abefh</sup>	877.12 ± 71.16 <sup>abefh</sup>	592.94 ± 36.39 <sup>abcdefh</sup>
SR	Left	538.80 ± 34.60	524.10 ± 28.28	523.06 ± 35.25	540.84 ± 29.81	501.11 ± 26.33	537.13 ± 28.67
	Right	525.39 ± 30.95	542.13 ± 37.73	524.73 ± 36.69	540.51 ± 29.39	523.44 ± 36.45	535.46 ± 32.57

Data expressed as mean ± SD.

<sup>a</sup> Compared with T<sub>0</sub>, P < 0.01; <sup>b</sup> compared with T<sub>1</sub>, P < 0.01; <sup>c</sup> compared with T<sub>2</sub>, P < 0.01; <sup>d</sup> compared with T<sub>3</sub>, P < 0.01; <sup>e</sup> compared with T<sub>4</sub>, P < 0.01; <sup>f</sup> compared with group C, P < 0.05; <sup>g</sup> compared with group SL, P < 0.05; <sup>h</sup> compared with group SR, P < 0.05; <sup>\*</sup> compared with the left side, P < 0.05; <sup>#</sup> compared with the right side, P < 0.05. CCBF, cerebral cortical blood flow; T<sub>0</sub>, baseline; T<sub>1</sub>, 10 min after SGB; T<sub>2</sub>, 30 min after SGB; T<sub>3</sub>, 60 min after SGB; T<sub>4</sub>, 90 min after SGB; T<sub>5</sub>, 120 min after SGB.

T<sub>2</sub> vs. T<sub>3</sub>, P = 0.002 for T<sub>2</sub> vs. T<sub>4</sub>). There were no significant differences in CCBF between T<sub>3</sub> and T<sub>4</sub> (P = 0.30), while it was significantly higher at T<sub>2</sub> than at T<sub>5</sub> (P < 0.001). These trends are depicted in Figures 6–9.

## Discussion

In this study, considering ptosis as a sign of successful block, we established the SGB model of C57BL/6 adult mice and measured bilateral CCBF at various time points before and after SGB. To our knowledge, we herein report a novel finding that unilateral SGB could produce similar effects on bilateral CCBF, which manifests as a transient decrease followed by a continuous increase for at least 2 h.

The stellate ganglion is usually merged by the inferior cervical ganglion and the T1–T3 thoracic sympathetic ganglia. The left and right stellate ganglia of the mice are both located anterior to the junction between the longus colli and the first rib. The stellate ganglion and

the sympathetic chain are both visible as white structures. The morphology and size of the stellate ganglion varies in mice, with the length of 0.7–1.5 mm and the width of approximately 0.3 mm<sup>[8]</sup>. In the present study, we selected the C7 spinous process as the positioning mark and inserted the needle closely along the lateral edge of C7 vertebral body toward the stellate ganglion. The local anesthetic was confined to the stellate ganglion by slow injection. A stable SGB mouse model was established with Horner's syndrome appearing in all the model mice.

One of the main factors regulating cerebral blood flow is the regulation of the cerebrovascular tension by the sympathetic nervous system. Cerebral blood vessels, particularly meningeal blood vessels, are widely innervated by noradrenergic sympathetic postganglionic fibers that originate from cervical sympathetic ganglia. The noradrenergic sympathetic postganglionic fibers move along the internal and external carotid arteries and

vertebral arteries and are distributed into the cranium. SGB can inhibit the activity of central and peripheral sympathetic nerves to relieve the extent of pathological augments of sympathetic activity and restore homeostasis. This makes it have certain therapeutic advantages on relieving cerebral vasospasms<sup>[9]</sup>. Gupta et al.<sup>[10]</sup> and Wendel et al.<sup>[11]</sup> used transcranial doppler for measuring the blood flow of the middle cerebral artery and found that SGB could reduce the tension of cerebral blood vessels on the blocked side, increase cerebral perfusion, and decrease the blood flow velocity. In addition, other studies have also confirmed the beneficial effects of SGB in neurosurgery patients<sup>[12]</sup>. SGB can relieve cerebral vasospasm in patients with subarachnoid hemorrhage and improve cerebral perfusion<sup>[13]</sup>.

In this study, we found that CCBF decreased transiently at 10 min after SGB, which is contrary to the previous viewpoint that SGB could only expand cerebral blood vessels and increase the blood flow on the blocked side<sup>[10]</sup>. In an earlier experimental study in rats, the brain blood vessels responded to electrical stimulation of cervical sympathetic nerves as contraction, which manifested as regional difference with the supply territory of the posterior communicating, middle cerebral, and posterior cerebral arteries being most prominent<sup>[14]</sup>. The cerebral blood vessels may contract when the cervical sympathetic nerve is stimulated. In the current study, the transient decrease of the CCBF after SGB may be attributed to the stimulation of the cervical sympathetic nerve by SGB manipulation; moreover, it may also signify a defensive reaction of the sympathetic nervous system to hyperperfusion<sup>[15]</sup>.

An indispensable part of our study is to explore the effect of unilateral SGB on the CCBF of the non-blocked side. We found that bilateral CCBF showed consistent trends after unilateral SGB, manifesting as a transient decrease followed by a continuous increase for at least 2 h, which is different from previous studies. Yokoyama et al.<sup>[12]</sup> concluded that SGB could increase the cerebral blood flow of the blocked side in patients with peripheral facial palsy while having no significant effect on the non-blocked side. In a study on 19 healthy female volunteers, Kang et al.<sup>[16]</sup> found that SGB had the following effects. It expanded the ipsilateral external carotid artery and its downstream branches (the superficial temporal artery and the occipital artery). It expanded the ophthalmic artery, a branch of internal carotid artery. It had no effect on the contralateral internal carotid artery and its branches (the ophthalmic artery and middle cerebral ar-

tery) or the ipsilateral and contralateral basilar arteries. Conversely, it contracted the ipsilateral middle cerebral artery and ipsilateral and contralateral posterior cerebral arteries, suggesting that the perivascular nerves and sympathetic nerves differently regulate intracranial and extracranial vasomotor centers.

Previous studies suggested that SGB increases the regional oxygen saturation ( $rSO_2$ ) on the blocked side and decrease it on the non-blocked side<sup>[17, 18]</sup>. In a study, the  $rSO_2$  of the non-blocked side was reported to level with that of the blocked side after inhaling oxygen 5 L/min for 5 min via a nasal cannula<sup>[18]</sup>. Jin et al.<sup>[19]</sup> concluded that SGB had no significant effects on intraoperative  $rSO_2$  in women undergoing breast cancer surgery. In the above three studies<sup>[17–19]</sup>, near-infrared spectroscopy (NIRS)-based  $rSO_2$  monitoring was used to study cerebral blood flow. This monitoring technique measures hemoglobin oxygen saturation in capillaries, arteries, and veins, but it cannot differentiate between arterial and venous blood vessels. Typically, about 75% of the cerebral blood flow to the brain tissues comes from the venous system and the rest comes from arteries and capillaries. Therefore, although  $rSO_2$  can reveal whether the regional cerebral oxygen supply and demand are balanced or not, it cannot provide information about oxygen delivery or be an indicator of cerebral blood flow. In previous studies, there has been no consensus on the effect of SGB on cerebral blood flow oxygenation through  $rSO_2$  monitoring. In our study, a laser speckle imaging system was used to measure the CCBF in mice. This system is a promising, minimally invasive, high-resolution optical technology and can quantify hemodynamic changes in real time with excellent spatial and temporal resolution<sup>[20]</sup>. This imaging system was first applied to detect the CCBF in rodents<sup>[21]</sup>, and the covered tissue, such as the rat skull, needs to be removed during detection. However, as the skull bones of C57BL/6 mice are thinner and have a higher transmission rate of the laser used for detection, CCBF imaging can be performed while keeping the mouse skull intact. In this study, bilateral CCBF continued to increase significantly for at least 2 h after a transient decrease, which may be attributed to the increase in cardiac output caused by the increase in heart rate and blood pressure after SGB. The results of a study evaluating the effects of SGB on heart rate and blood pressure changes in patients showed that blood pressure and heart rate increased significantly at 10 and 15 min after SGB<sup>[17]</sup>. In groups L and R, the degree of decrease in CCBF was significantly lower on the unblocked

side than on the blocked side at  $T_1$ , which needs further investigation.

We found that the eyelids may not manifest ptosis when mice get increasingly alert. This phenomenon may be related to the excitement compensation of sympathetic nerves. In this study, we placed the mice in a transparent rearing cage to reduce their alertness. During model establishment, the limbs of the mice were well stretched and fixed, which can increase the success rate of the SGB while causing fewer complications.

The present study has several limitations. First, the alertness of mice and the diversity of their activities make the observation of ptosis difficult and may also lead to inaccurate timing judgment of ptosis symptoms. Second, we did not monitor the changes in the temperature of mice limbs to further clarify the success rate of SGB; however, there has been an earlier clinical report wherein the success rate of SGB was reportedly inconsistent with the increase in the skin temperature of the ipsilateral upper extremity<sup>[22]</sup>, which has not been confirmed in mice. Third, during model establishment, we did not monitor blood pressure and heart rate to study the regulatory effect of SGB on the cardiovascular system and the corresponding impact on CCBF. Finally, we only detected the CCBF within 120 min after SGB. In the future, more research investigating the influence of SGB on brain tissue perfusion under normal and pathological conditions is warranted.

## Conclusion

In conclusion, we established the SGB model of C57BL/6 adult mice through percutaneous posterior approach and reported novel findings of unilateral SGB exerting similar effects on bilateral CCBF, manifesting as a transient decrease followed by a continuous increase for at least 2 h.

## Authors' Contributions

Jiahua Wang responsible for conceptualization, methodology, formal analysis, writing-original draft, project administration. Wei Zhou responsible for conceptualization, methodology, formal analysis, writing-original draft. Xiaohong Wang responsible for conceptualization, methodology, resources. Shiting Yan responsible for Investigation, formal analysis, writing-original draft. Shunping Tian responsible for Investigation. Ying Wang responsible for Investigation. Yanlong Yu

responsible for formal analysis. Hu Li responsible for formal analysis. Dongsheng Zhang responsible for formal analysis. Zhang Zhuan responsible for conceptualization, methodology, writing-original draft visualization, supervision, writing-review&editing, funding acquisition. All authors read and approved the final manuscript.

## Acknowledgements

We sincerely thank all the staff in the Anatomy Department of School of Medicine of Yangzhou University for their help during this study.

## References

1. Kim YH, Kim SY, Lee YJ, Kim ED. A Prospective, Randomized Cross-Over Trial of T2 Paravertebral Block as a Sympathetic Block in Complex Regional Pain Syndrome. *Pain Physician* [Internet]. 2019;22(5):E417-E424. Available from: <https://pubmed.ncbi.nlm.nih.gov/31561653/>
2. Lipov EG, Joshi JR, Sanders S, Wilcox K, Lipov S, Xie H, et al. Effects of stellate-ganglion block on hot flushes and night awakenings in survivors of breast cancer: a pilot study. *The Lancet Oncology* [Internet]. 2008 Jun;9(6):523–32. Available from: [http://dx.doi.org/10.1016/s1470-2045\(08\)70131-1](http://dx.doi.org/10.1016/s1470-2045(08)70131-1)
3. Wu C-N, Wu X-H, Yu D-N, Ma W-H, Shen C-H, Cao Y. A single-dose of stellate ganglion block for the prevention of postoperative dysrhythmias in patients undergoing thoracoscopic surgery for cancer. *European Journal of Anaesthesiology* [Internet]. 2020 Apr;37(4):323–31. Available from: <http://dx.doi.org/10.1097/eja.0000000000001137>
4. Rae Olmsted KL, Bartoszek M, Mulvaney S, McLean B, Turabi A, Young R, et al. Effect of Stellate Ganglion Block Treatment on Posttraumatic Stress Disorder Symptoms. *JAMA Psychiatry* [Internet]. 2020 Feb 1;77(2):130–8. Available from: <http://dx.doi.org/10.1001/jamapsychiatry.2019.3474>
5. Abdi S, Yang Z. A Novel Technique for Experimental Stellate Ganglion Block in Rats. *Anesthesia & Analgesia* [Internet]. 2005 Aug;101(2):561–5. Available from: <http://dx.doi.org/10.1213/01.ane.0000159169.12425.50>
6. Gulcu N, Gonca E, Kocoglu H. A Lateral Percutaneous Technique for Stellate Ganglion Blockade in Rats. *Anesthesia & Analgesia* [Internet]. 2009 May;108(5):1701–4. Available from: <http://dx.doi.org/10.1213/01.ane.0000347419.62425.50>

- org/10.1213/ane.0b013e31819c6018
7. Ogo S, Tarumi T. Cerebral blood flow regulation and cognitive function: a role of arterial baroreflex function. *The Journal of Physiological Sciences* [Internet]. 2019 Aug 23;69(6):813–23. Available from: <http://dx.doi.org/10.1007/s12576-019-00704-6>
  8. Scherschel K, Bräuninger H, Glufke K, Jungen C, Klöcker N, Meyer C. Location, Dissection, and Analysis of the Murine Stellate Ganglion. *Journal of Visualized Experiments* [Internet]. 2020 Dec 22;(166). Available from: <http://dx.doi.org/10.3791/62026>
  9. Zhang J, Nie Y, Pang Q, Zhang X, Wang Q, Tang J. Effects of stellate ganglion block on early brain injury in patients with subarachnoid hemorrhage: a randomised control trial. *BMC Anesthesiology* [Internet]. 2021 Jan 20;21(1):23. Available from: <http://dx.doi.org/10.1186/s12871-020-01215-3>
  10. Gupta MM, Bithal PK, Dash HH, Chaturvedi A, Mahajan RP. Effects of stellate ganglion block on cerebral haemodynamics as assessed by transcranial Doppler ultrasonography. *British Journal of Anaesthesia* [Internet]. 2005 Nov;95(5):669–73. Available from: <http://dx.doi.org/10.1093/bja/aei230>
  11. Wendel C, Scheibe R, Wagner S, Tangemann W, Henkes H, Ganslandt O, Schiff JH. Decrease of blood flow velocity in the middle cerebral artery after stellate ganglion block following aneurysmal subarachnoid hemorrhage: a potential vasospasm treatment? *J Neurosurg* [Internet]. 2019 Aug 9;1-7. Available from: <http://dx.doi.org/10.3171/2019.5.JNS182890>
  12. Yokoyama K, Kishida T, Sugiyama K. Stellate ganglion block and regional cerebral blood volume and oxygenation. *Canadian Journal of Anesthesia/Journal canadien d'anesthésie* [Internet]. 2004 May;51(5):515–6. Available from: <http://dx.doi.org/10.1007/bf03018319>
  13. Treggiari MM, Romand J-A, Martin J-B, Reverdin A, Rüfenacht DA, de Tribolet N. Cervical Sympathetic Block to Reverse Delayed Ischemic Neurological Deficits After Aneurysmal Subarachnoid Hemorrhage. *Stroke* [Internet]. 2003 Apr;34(4):961–7. Available from: <http://dx.doi.org/10.1161/01.str.0000060893.72098.80>
  14. Tuor UI. Local distribution of the effects of sympathetic stimulation on cerebral blood flow in the rat. *Brain Research* [Internet]. 1990 Oct;529(1–2):224–31. Available from: [http://dx.doi.org/10.1016/0006-8993\(90\)90831-u](http://dx.doi.org/10.1016/0006-8993(90)90831-u)
  15. Cassaglia PA, Griffiths RI, Walker AM. Sympathetic Withdrawal Augments Cerebral Blood Flow During Acute Hypercapnia in Sleeping Lambs. *Sleep* [Internet]. 2008 Dec;31(12):1729–34. Available from: <http://dx.doi.org/10.1093/sleep/31.12.1729>
  16. Kang C-K, Oh S-T, Chung RK, Lee H, Park C-A, Kim Y-B, et al. Effect of Stellate Ganglion Block on the Cerebrovascular System. *Anesthesiology* [Internet]. 2010 Oct 1;113(4):936–44. Available from: <http://dx.doi.org/10.1097/aln.0b013e3181ec63f5>
  17. Park HM, Kim TW, Choi HG, Yoon KB, Yoon DM. The Change in Regional Cerebral Oxygen Saturation after Stellate Ganglion Block. *The Korean Journal of Pain* [Internet]. 2010 Jun 30;23(2):142–6. Available from: <http://dx.doi.org/10.3344/kjp.2010.23.2.142>
  18. Kim EM, Yoon KB, Lee JH, Yoon DM, Kim DH. The effect of oxygen administration on regional cerebral oxygen saturation after stellate ganglion block on the non-blocked side. *Pain Physician* [Internet]. 2013 Mar-Apr;16(2):117–24. Available from: <https://pubmed.ncbi.nlm.nih.gov/23511678/>
  19. Jin F, Li X, Tan W, Ma H, Fang B, Tian A, et al. Effects of ultrasound-guided stellate-ganglion block on sleep and regional cerebral oxygen saturation in patients undergoing breast cancer surgery: a randomized, controlled, double-blinded trial. *Journal of Clinical Monitoring and Computing* [Internet]. 2018;32(5):855–62. Available from: <http://dx.doi.org/10.1007/s10877-017-0074-3>
  20. Du E, Shen S, Chong SP, Chen N. Multifunctional laser speckle imaging. *Biomedical Optics Express* [Internet]. 2020 Mar 13;11(4):2007–16. Available from: <http://dx.doi.org/10.1364/boe.388856>
  21. Durduran T, Burnett MG, Yu G, Zhou C, Furuya D, Yodh AG, et al. Spatiotemporal Quantification of Cerebral Blood Flow during Functional Activation in Rat Somatosensory Cortex using Laser-Speckle Flowmetry. *Journal of Cerebral Blood Flow & Metabolism* [Internet]. 2004 May;24(5):518–25. Available from: <http://dx.doi.org/10.1097/00004647-200405000-00005>
  22. Stevens RA, Stotz A, Kao TC, Powar M, Burgess S, Kleinman B. The relative increase in skin temperature after stellate ganglion block is predictive of a complete sympathectomy of the hand. *Regional Anesthesia and Pain Medicine* [Internet]. 1998 May;23(3):266–70. Available from: [http://dx.doi.org/10.1016/s1098-7339\(98\)90053-0](http://dx.doi.org/10.1016/s1098-7339(98)90053-0)

**Створення моделі на миші — блокади зірчастого ганглія та наступних двофазних впливів на двосторонній церебральний кортикальний кровотік**

Jiahua Wang<sup>1</sup>, Wei Zhou<sup>1,2,3</sup>, Xiaohong Wang<sup>1</sup>, Shiting Yan<sup>2</sup>, Shunping Tian<sup>1,2,3</sup>, Ying Wang<sup>1</sup>, Yanlong Yu<sup>1,3</sup>, Hu Li<sup>1,2</sup>, Dongsheng Zhang<sup>1,3</sup>, Zhuan Zhang<sup>1</sup>

<sup>1</sup>Affiliated Hospital of Yangzhou University, Yangzhou University, Yangzhou, China;

<sup>2</sup>School of Medicine, Yangzhou University, Yangzhou, China;

<sup>3</sup>Dalian Medical University, Dalian, China

Джерела фінансування: це дослідження було підтримано Проектом підготовки ключових медичних талантів Комісії з питань охорони здоров'я та планування сім'ї міста Янчжоу (ZDRC201815) і Ключовою програмою дослідницького гранту Афілійованої лікарні університету Янчжоу (YZYY2017-07).

Конфлікт інтересів: Автори заявляють, що не мають конфлікту інтересів.

**Анотація**

**Передумови та мета:** блокада зірчастого ганглія (SGB) має значну терапевтичну ефективність у різних клінічних практиках, тому необхідні подальші дослідження SGB. Модель SGB на миші не було описано, і вплив на церебральний кортикальний кровотік (CCBF) був суперечливим. Ми мали на меті створити модель блокади зірчастого ганглія (SGB) на миші і дослідити, як SGB впливає на CCBF.

**Методи:** самців мишей C57BL/6 випадковим чином розділили на п'ять груп (n = 6): групи L (лівий SGB) і R (правий SGB) отримували ін'єкцію 0,25 % ропівакаїну гідрохлориду (0,08 мл) у відповідний зірчастий ганглії; так само групи SL (лівий контроль фізіологічного розчину) і SR (правий контроль фізіологічного розчину) замість цього отримували ін'єкцію нормального фізіологічного розчину (0,08 мл). Група C не отримувала втручання. CCBF оцінювали до SGB (T0) і через 10 (T1), 30 (T2), 60 (T3), 90 (T4) і 120 хвилин (T5) після SGB з використанням лазерної спекл-контрастної системи візуалізації.

**Результати:** модель SGB на миші була успішно створена в групах L і R. Порівняно з базовим рівнем, CCBF на стороні блокування знизився на T1, збільшився на T2–T5 і досяг піку на T3 у групах L і R (усі, P < 0,01). Порівняно з групами C і SL, CCBF з лівого боку знизився на T1 і збільшився на T2–T5 у групі L (усі, P < 0,05). Подібна тенденція була відмічена в групах C і SR відносно групи R. CCBF на заблокованій стороні знизився на T1, збільшився на T2–T5 і досяг піку на T3 у групах L і R (усі, P < 0,01).

**Висновки:** модель SGB на миші була створена успішно. Однобічний SGB може впливати на двобічний церебральний кортикальний кровотік, який демонструє тимчасове зниження з наступним значним збільшенням протягом щонайменше 2 годин.

**Ключові слова:** блокада зірчастого ганглія; модель на миші; церебральний кровотік; симпатична нервова система